Radiative ballistic phonon transport in silicon-nitride membranes at low temperatures

H. F. C. Hoevers,[a] M. L. Ridder, A. Germeau, M. P. Bruijn, and P. A. J. de Korte
SRON National Institute for Space Research, Sorbonnelaan 2, 3584 CA Utrecht, The Netherlands

R. J. Wiegerink
MESA$^+$ *Institute, University of Twente, P.O. Box 217, 7500 AE Enschede, The Netherlands*

(Received 21 February 2005; accepted 11 May 2005; published online 13 June 2005)

We studied the phonon transport in free-standing 1 μm thick silicon-nitride membranes at temperatures around 100 mK. By varying the geometry of the membranes and the dimensions of the heater element, we are able to distinguish between radiative and diffuse phonon transport. The data indicate that the transport is radiative ballistic with a lower limit to a phonon mean-free path of about 1 mm and that the probability for specular reflection from the surface is at least 0.99. The tested silicon-nitride membranes were grown on Si(100), Si(110), and polycrystalline-Si and the transport properties show no dependency on the substrate. © *2005 American Institute of Physics*. [DOI: 10.1063/1.1949269]

Free-standing low-stress silicon-rich nitride (Si_xN_y) membranes are commonly used in bolometric and calorimetric sensors to support individual sensor pixels with a well-defined thermal coupling to the heat bath.[1,2] The thermal conductance of each pixel to the bath is a primary design parameter, controlling the thermal time constant of the detector.

The power flow from sensor to bath at temperature T and T_{bath}, respectively, can be expressed as $P=K(T^n-T_{\mathrm{bath}}{}^n)$, implying a thermal conductance $G=nKT^{n-1}$ for the thermal link. Until now, the thermal transport in Si_xN_y membranes at low temperatures was interpreted in terms of diffuse phonon transport[3,4] with the geometry dependent factor K in the heat conductance G_{dif} equal to $K=\alpha A/(Ln)$, with A and L as the cross section and length of the thermal link, respectively, and α as the specific heat conductance of Si_xN_y. The material parameters α and n can be determined by measuring P as function of T_{bath}; for our membranes, we consistently find $n\approx 3.6$. The value of α was, however, found to be geometry dependent, indicating that the heat transport cannot be described by diffuse transport.

Radiative phonon transport has been suggested as transport mechanism[4,5] with $P_{\mathrm{rad}}=\sigma A_{\mathrm{ph}}\xi(T^4-T_{\mathrm{bath}}^4)$ and $G_{\mathrm{rad}}=4\sigma A_{\mathrm{ph}}\xi T^3$; here $\sigma=157\ \mathrm{W\,m^{-2}\,K^{-4}}$ is the Stefan Boltzmann constant for two transverse and one longitudinal acoustic mode in Si_xN_y, A_{ph} is the phonon-emitting area, and the factor ξ describes the transport efficiency. If $\xi=1$, the phonon transport is ballistic with specular reflections from the surface. The Casimir limit[6] gives a lower limit to ξ for complete diffuse surface scattering. Although Ref. 4 stresses radiative phonon transport, the thermal conductivity was subsequently interpreted in terms of diffuse transport. In this letter, the geometrical dependencies of G_{dif} and G_{rad} are explored which will allow us to discriminate between diffuse and radiative transport.

We measured the power flow from a heater element through a Si_xN_y membrane to a heat bath (at 20 mK) consisting of a Si chip cooled by a dilution refrigerator. In the experiments, a superconducting to normal phase transition edge sensor[2] (TES) is used as heater element. The TES is voltage biased and will, as a result of its internal negative electrothermal feedback, self-stabilize in the superconducting transition at a resistance R_{TES}. The power flow from the TES to the heat bath equals $P_{\mathrm{Joule}}=V^2/R_{\mathrm{TES}}=K(T^n-T_{\mathrm{bath}}^n)$ and is (almost) independent of R_{TES}. In our experiments, the TES is a TiAu bilayer deposited on a Si_xN_y membrane with Ti and Au thicknesses of 14 and 50 nm, respectively, and has a critical (i.e., operating) temperature $T\sim$ 85 mK. Inside the TES, the electron-phonon coupling poses a limit to the maximum power flow. We calculate $P_{\text{el-ph}}=V\Sigma_{\mathrm{TiAu}}(T^n-T_{\mathrm{bath}}^n)=19$ pW at $T=85$ mK for a typical TES of $V=160\times 160\ \mu\mathrm{m}^2\times 64$ nm. The material parameters $\Sigma_{\mathrm{TiAu}}=(5.5\pm 1.3)10^9\ \mathrm{W\,K^{-5.3}\,m^{-3}}$ and $n=5.3$ were experimentally derived for our TiAu TESs and are in accordance with data from literature.[7] In addition, we estimate that the Kapitza coupling between the phonons in the TES and the substrate,[8] $P_{\mathrm{Kap}}=A_{\mathrm{TES}}\Sigma_{\mathrm{Kap}}(T^4-T_{\mathrm{bath}}^4)$, allows for a power flow from the TES to the Si_xN_y membrane of about 166 pW (with $A_{\mathrm{TES}}=160\times 160\ \mu\mathrm{m}^2$ and $\Sigma_{\mathrm{Kap}}=125\ \mathrm{W\,K^{-4}\,m^{-2}}$). In our experiments, $P_{\text{el-ph}}$ and P_{Kap} are always larger than P_{Joule} implying that the phonons in the Si_xN_y below the TES are in thermal equilibrium with the electrons in the TES. The low-stress silicon-rich nitride membranes, grown by low pressure chemical vapor deposition on Si(100), Si(110), and polycrystalline-Si (poly-Si) substrates used in the experiments, were produced at the MESA$^+$ facility.

In Geometry 1, the TES is deposited on a closed Si_xN_y membrane grown on a Si(110) substrate. The length of the membrane is 1.3 mm and the width is varied in the experiments from 140 to 210 μm. As the dimensions of the TES are kept constant, the distance L between the TES and the Si beam varies (see Fig. 1). Assuming diffuse transport, the principal power flow from the TES to the Si beams is: $P_{\mathrm{dif}}=2\alpha A/(Ln)(T^n-T_{\mathrm{bath}}^n)$ with A equal to $L_{\mathrm{TES}}\times Si_xN_y$-thickness$=160\times 1\ \mu\mathrm{m}^2$. If the transport is radiative, the power flows in all four directions and the phonon-emitting area is equal to the product of the circumference of the TES and the Si_xN_y thickness: $A_{\mathrm{ph}}=4\times 160\times 1\ \mu\mathrm{m}^2$. It is predicted that P_{dif} will depend on L, whereas P_{rad} is independent

[a]Electronic mail: h.hoevers@sron.nl

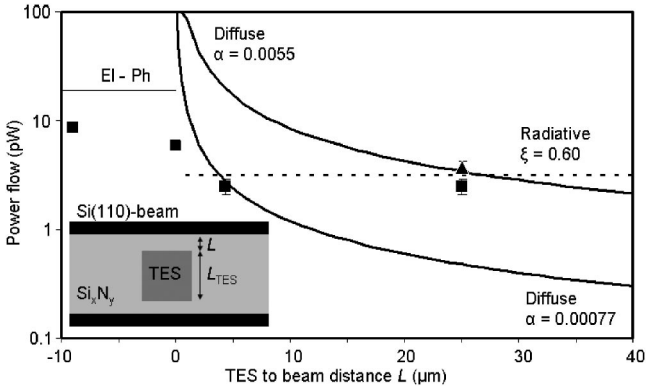

FIG. 1. The TES to beam distance L is varied (see inset, the Si_xN_y membrane extends further to the right and left where it also connects to the heat bath, not shown) and the power flow from the TES to the Si beams is measured. The data are from wafer M120 (squares) and M55 (triangle, $T=88$ mK). The curved lines assume diffuse transport with $\alpha=0.0055$ and $\alpha=0.00077$ W $K^{-3.6}$ m^{-1}. The horizontal dashed line assumes radiative transport with $\xi=0.60$. For negative values of L, a pixel overlaps on the Si beam; the line at 19 pW is the maximum power flow ($P_{el\text{-}ph}$) for a TES on a solid substrate.

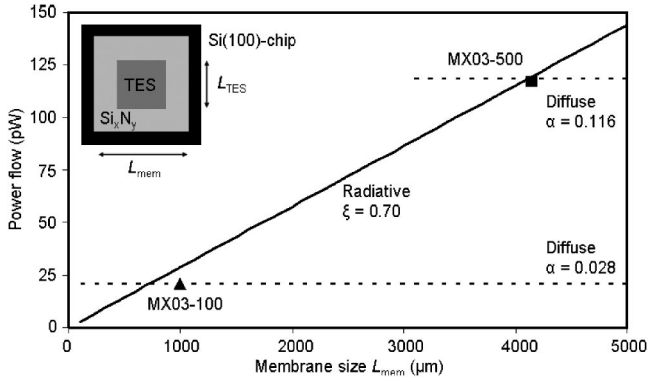

FIG. 2. In Geometry 2, the TES and membrane size are varied while their ratio (L_{mem}/L_{TES}) is kept constant at about 10 (see the inset) and the power flow from the TES to the Si chip is measured. The dashed lines are calculated assuming diffuse phonon transport for $L_{mem}/L_{TES}=10$ and $\alpha=0.028$ W $K^{-3.6}$ m^{-1}, respectively, $L_{mem}/L_{TES}=8$ and $\alpha=0.116$ W $K^{-3.6}$ m^{-1}. The solid line assumes radiative phonon transport with $\xi=0.70$ and $L_{mem}/L_{TES}=10$. MX03-100 and MX03-500 have $T=146$ and 159 mK, respectively.

of L. Test structures were produced from the same Si_xN_y wafer and with the same TiAu bilayer (M120 with $T=85$ m K, see Fig. 1). If the data are analyzed assuming diffuse transport with $n=3.6$, we derive $\alpha=0.000\,77$ W $K^{-3.6}$ m^{-1} for the $L=4.3$ μm data point and $\alpha=0.0055$ W $K^{-3.6}$ m^{-1} for both $L=25$ μm data points. Since α changes by a factor of 7 with geometry, it is obviously not a true material parameter. The same data are also analyzed assuming radiative phonon transport and fit well for $\xi=0.60$. The data point in Fig. 1 at $L=0$ μm refers to the situation in which the TES starts to overlap the Si beam; for $L=-10$ μm, the TES overlaps the Si beam 10 μm on both sides. The power flow for $L=-10$ μm increases as the cross section for the heat flow increases and will ultimately be limited by $P_{el\text{-}ph}$ (this limit is not yet reached in the experiments shown). The two fits in Fig. 1 assume diffuse transport and predict a sharp increase of the power flow for $L=0$ μm which is not measured.

In Geometry 2, the TES is produced on a closed square membrane grown on a Si(100) substrate. In the experiments, the dimensions of the square TES (L_{TES}) and membrane (L_{mem}) are varied but their ratio is kept constant. For diffuse phonon transport, the power flow is calculated assuming a circular geometry: $P_{dif}=2\pi t\alpha/[\ln(r_{mem}/r_{TES})n](T^n-T_{bath}^n)$ where the radii r_{TES} and r_{mem} of the TES and membrane are approximated by $\pi {r_{TES}}^2={L_{TES}}^2$ and $\pi {r_{mem}}^2={L_{mem}}^2$ and t is the membrane thickness. In the case of radiative phonon transport, $P_{rad}=\sigma A_{ph}(T^4-T_{bath}^4)\xi$, with the phonon-emitting area $A_{ph}=2tr_{TES}$. Two test structures were produced from the same Si_xN_y wafer and with the same TiAu bilayer as heater and measured (see Fig. 2). The structures have a comparable L_{mem}/L_{TES} ratio of 8, respectively, 10, for MX03-500 and MX03-100 so diffuse phonon transport predicts comparable values of P_{dif} while radiative phonon transport predicts a larger power flow for MX03-500 as it has a five times larger L_{TES} than MX03-100. If the data of MX03-100 and MX03-500 are analyzed assuming diffuse phonon transport with $n=3.6$, α equals 0.028, respectively, 0.116 W $K^{-3.6}$ m^{-1}, again confirming that α is not constant and that the transport is not diffuse. In contrast, both measurements can be described assuming radiative phonon transport with $\xi=0.70$.

A more extensive data set was also compiled and includes an additional measurement at $T=120$ mK for Geometry 1 and five more data sets at $T\sim100$ mK for Geometry 2, collected over a period of about five years and from different wafers. These additional data are consistent with the previously presented data. In the new Geometry 3, the TESs are connected to the heat bath through four etched support legs rather than a closed membrane. The length of the support legs ranges from 10 to 25 μm and their width is varied from 15 to 60 μm. The samples in Geometry 3 use Si_xN_y grown on Si(100), Si(110), and poly-Si and were analyzed like the data for Geometry 1 and 2. Figure 3 combines all experimental data and shows that the parameter α (assuming diffuse transport) appears to vary up to two orders of magnitude. The same data, analyzed assuming radiative phonon transport, can be described with $\xi=0.78\pm0.18$. The value of ξ also indicates that there is no major (if any) relation between the thermal transport of the Si_xN_y and the orientation of the Si substrate. The error bars in Fig. 3 are estimated from the measurement accuracy of P_{Joule} and T (typically 0.3 pW and 3 mK, respectively). In the following section, we assume the phonon transport to be radiative and discuss the derived

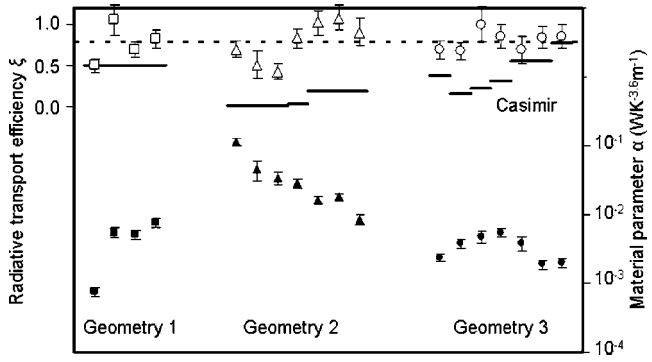

FIG. 3. Thermal data analyzed assuming diffuse phonon transport (filled symbols, right axis) and radiative phonon transport (open symbols, left axis). The dashed line indicates radiative transport with $\xi=0.78$; the horizontal lines indicate the Casimir limit to ξ. The data of Geometry 2 are arranged in order of decreasing membrane dimensions starting from 4000 μm (left) down to 440 μm (right).

value of ξ, as well as details of the phonon transport.

The transport in the studied Si_xN_y structures can be described with $\xi=0.78\pm0.18$ (Fig. 3). This estimate of ξ uses a simple geometrical model for the phonon-emitting area and assumes that the Si chip acts as a perfect absorber of heat. A more elaborate geometrical modeling will lead to more accurate values of ξ. Moreover, ξ is directly dependent on the Stefan–Boltzmann constant σ (used to calculate the expected power flow) which, in turn, depends on the speed of sound in Si_xN_y. A 5% larger value of the average speed of sound already leads to a 10% larger value of ξ. Accounting, for the simplicity of the modeling, the obtained value and accuracy of ξ are very reasonable and it is emphasized that the value of ξ is applicable for transport in Si_xN_y structures with sizes ranging from 10 μm (in Geometry 1 and 3) up to several mm size (in Geometry 2). The lower limit to ξ is the Casimir limit:[6] $\xi_{\text{Casimir}}\approx A^{1/2}/L$. The Casimir limit is calculated and plotted in Fig. 3 for all samples. As can be seen, $\xi>\xi_{\text{Casimir}}$ for almost all our samples, and certainly for the samples in which the largest Si_xN_y dimensions are involved (Geometry 2); assuming Λ to be large, it is concluded that the surface reflections are predominantly be specular.

So far, only the average phonon transport efficiency (described with ξ) has been considered. In the following discussion, ξ is related to the microscopic transport parameters, i.e., the probability σ_{ph} for a phonon to reflect specularly from the surface and the phonon mean-free path Λ. The probability $P(d)$ for a phonon to travel a distance d from an emitter without being diffusely scattered is:[9] $P(d)=\exp[\ln(\sigma_{\text{ph}})\sin(\theta)(d/t)-d/\Lambda]$, with the phonon emitted at an angle θ with respect to the plane of the membrane. Since our data are not in the Casimir limit, an appreciable value of $P(d)$ is expected. We analyze the data of MX03-500 (having $d\approx2$ mm) since this sample involves the longest length scales and is most sensitive to scattering. Although arbitrarily chosen, we first set $P(d)>0.1$ and calculate that $P(d=2\text{ mm})>0.1$ requires $\sigma_{\text{ph}}>0.99$ (for $d/\Lambda=0$), respectively, $\Lambda>0.9$ mm (for $\sigma_{\text{ph}}=1$), assuming an isotropic point source as an emitter. As indicated, $P(d)>0.1$ is arbitrarily chosen and $P(d=2\text{ mm})>0.8$ would require $\sigma_{\text{ph}}>0.9997$ (for $d/\Lambda=0$), respectively, $\Lambda>9$ mm (for $\sigma_{\text{ph}}=1$). From these numbers, we estimate a lower limit to the probability of specular reflection of $\sigma_{\text{ph}}\approx0.99$ and to the phonon mean-free path of $\Lambda\approx1$ mm. The probability of specular reflection from the surface[9,10] can also be estimated from the root-mean-square surface roughness η and the phonon wave number q: $\sigma_{\text{ph}}=\exp(-4\pi\eta^2q^2)$. Atomic force microscopy of very similar[11] Si_xN_y layers indicates $\eta\approx3$ nm, while the membrane thickness will determine $q\approx2\pi/t$. This leads to $\sigma_{\text{ph}}=0.996$ which is in agreement with the lower limit to σ_{ph} estimated from the thermal transport properties.

The implications of the radiative ballistic nature of the phonon transport in the design of radiation detectors are two fold. First, it should be accounted for in the thermal design of bolometers and microcalorimeters. It is especially relevant for the design of bolometers aiming at a very low noise equivalent power $[(4k_BT^2G)^{1/2}<10^{-18}\ \text{W/Hz}^{1/2}]$ optimized to detect sub-mm radiation. The low-G support structures for these detectors will require a proper geometrical design in combination with and low value of ξ that can be realized by using very long support structures and/or by roughening the Si_xN_y surface. The second implication of radiative ballistic transport is that the models used to predict the performance of bolometers and microcalorimeters account for a reduction of the phonon noise as result of a distributed temperature in the thermal link[12] by a factor of $\gamma=n/(2n+1)\approx0.5$. In the case of radiative ballistic transport, this temperature distribution is, however, absent and the noise and performance analysis should account for $\gamma=1$.

The authors thank J. van Baar and J.H. de Boer (MESA^+) for producing the Si_xN_y membranes and N. H. Baars, E. Krouwer, and T. Plomp (SRON) for experimental support. Part of this work is supported by a grant from the Dutch Organization for Scientific Research (NWO) and by Contract No. 15850/01/NL/HB of ESA's technological research program.

[1] P. L. Richards, J. Appl. Phys. **76**, 1 (1994).
[2] K. D. Irwin G. C. Hilton, D. A. Wollman, and J. M. Martinis, Appl. Phys. Lett. **69**, 1945 (1996).
[3] M. M. Leivo and J. P. Pekola, Appl. Phys. Lett. **72**, 1305 (1998).
[4] W. Holmes, J. M. Gildemeister, P. L. Richards, and V. Kotsubo, Appl. Phys. Lett. **72**, 2250 (1998).
[5] T. Klitsner, J. E. VanCleve, H. E. Fisher, and R. O. Pohl, Phys. Rev. B **38**, 7576 (1988).
[6] H. Casimir, Physica (Amsterdam) **5**, 495 (1938).
[7] F. C. Wellstood, C. Urbina, and J. Clarke, Phys. Rev. B **49**, 5942 (1994).
[8] F. Pröbst, M. Frank, S. Cooper, P. Colling, D. Dummer, P. Ferger, G. Forster, A. Nucciotti, W. Seidel, and L. Stodolsky, J. Low Temp. Phys. **100**, 69 (1995).
[9] D. V. Anghel, J. P. Pekola, M. M. Leivo, J. K. Suoknuuti, and M. Manninen, Phys. Rev. Lett. **81**, 2958 (1998).
[10] J. M. Ziman, *Electrons and Phonons: The Theory of Transport Phenomena in Solids* (Oxford University Press, New York, 1979).
[11] M. Elwenspoek and R. J. Wiegerink, *Mechanical Microsensors* (Springer, Berlin, 2001).
[12] J. C. Mather, Appl. Opt. **21**, 1125 (1982).